# Microplane Model M5 with Kinematic and Static Constraints for Concrete Fracture and Anelasticity. II: Computation

Zdeněk P. Bažant, F.ASCE,[1] and Ferhun C. Caner[2]

**Abstract:** Following the formulation of the constitutive model in the preceding Part I in this issue, the present Part II addresses the problems of computational algorithm and convergence of iterations. Typical numerical responses are demonstrated and the parameters of the model are calibrated by test data from the literature.

**DOI:** 10.1061/(ASCE)0733-9399(2005)131:1(41)

**CE Database subject headings:** Concrete; Fracture; Inelastic action; Damage; Softening; Finite element method; Numerical models.

## Introduction

After formulating the microplane constitutive model in the preceding Part I (Bažant and Caner 2005), we are now ready to introduce a localization limiter preventing spurious mesh sensitivity, develop the numerical algorithm, and investigate the conditions of convergence of iterations. Then we will demonstrate typical numerical simulations, compare the model to the characteristic test data from the literature, and calibrate the model parameters.

## Adjustment of Postpeak Softening Based on Fracture Energy

To prevent postpeak strain softening from causing spurious mesh sensitivity in finite element analysis, one may apply the crack band model (Bažant and Oh 1983), in which the energy dissipation per unit volume is adjusted according to the ratio of the element size $h$ to the characteristic crack bandwidth $l$ (a material length), so as to achieve mesh-indendent energy dissipation per unit area of the crack plane.

Postpeak strain softening is known to engender spurious mesh sensitivity in finite element analysis (Bažant 1976), with the energy dissipation per unit area of failure surface depending on the chosen finite element size. There are two expedient ways to avoid it: (1) on the constitutive level, by applying the crack band model (Bažant and Oh 1983), in which the energy dissipation per unit volume is adjusted according to the ratio of the element size $h$ to the characteristic crack bandwidth $l$ (a material length); and (2) on the finite element level, by using a composite finite element in which a softening finite element is coupled in three dimensions with unloading finite elements without adjusting the microplane constitutive law (Bažant et al. 2002, 2001b). The former, named Model M4f and developed by Bažant et al. (2002), is simpler and has been adopted for the present numerical studies. It may be briefly described as follows.

Width $l$ is the characteristic size of the representative volume (or characteristic length) of material for which the microplane constitutive model has been calibrated by tests (as described for M4 in Caner and Bažant 2000). The area $W_f$ under the postpeak softening portion of each microplane stress–strain curve, multiplied by $l$, represents a contribution to the fracture energy of the material, which must be a constant in order to avoid spurious mesh sensitivity (Bažant and Oh 1983). If element size $h=l$ is chosen, the energy dissipation will be correct without any adjustment of microplane constitutive laws. However, an adjustment is needed when $h \neq l$ because the strain softening tends to localize into a band of a single element width.

Energy equivalence requires the adjustment to be such that $W_f^* h = W_f l$ or $W_f^* = W_f l/h$, where $W_f^*$ is the area under the postpeak softening curve of each microplane stress–strain curve (Fig. 1). This may be achieved by a horizontal rescaling of all the softening boundaries, tensile as well as compressive, in the ratio $r = l/h$; see Fig. 1 where Point 2 represents the point at which the softening begins. Let Point $P$ be any point on the softening Boundary Curve 23, and let $U$ be a point at the same level (same stress) on the Unloading Line 10. The rescaling must be such that Point $P$ moves to Point $P'$ for which $\overline{UP'} = r\overline{UP}$. This represents a horizontal affinity transformation with respect to Axis 10, which transforms softening Boundary Curve 23 to a new softening Boundary Curve $2'3'$.

When the element is too large, ratio $r$ could be so small that the transformed softening curve exhibits a snapback, i.e., the slope at some points changes from negative to positive. Since static finite element analysis cannot cope with snapback instability, elements that large cannot be allowed.

For mathematical implementation it is somewhat inconvenient that the axis of affinity is inclined. Since the inclination is very steep compared to the slope of the softening boundary, it makes little difference if the inclined affinity Axis 24 is replaced by the vertical affinity Axis 45 such that the area 23012 be equal to the

[1]McCormick School Professor and W. P. Murphy Professor of Civil Engineering and Materials Science, Northwestern Univ., 2145 Sheridan Rd., Tech A135, Evanston, IL 60208. E-mail z-bazant@northwestern.edu

[2]Ramón y Cajal Fellow, ETSECCPB-ETCG, Univ. Politecnica de Catalunya, Jordi Girona 1-3, Ed.D2 D.305, Barclona 08034, Spain E-mail: ferhun.caner@upc.es; formerly, Visiting Scholar, Northwestern Univ., 2145 Sheridan Rd., Evanston, IL 60208.

Note. Associate Editor: Franz-Josef Ulm. Discussion open until June 1, 2005. Separate discussions must be submitted for individual papers. To extend the closing date by one month, a written request must be filed with the ASCE Managing Editor. The manuscript for this paper was submitted for review and possible publication on January 27, 2003; approved on February 13, 2004. This paper is part of the ***Journal of Engineering Mechanics***, Vol. 131, No. 1, January 1, 2005. ©ASCE, ISSN 0733-9399/2005/1-41–47/$25.00.

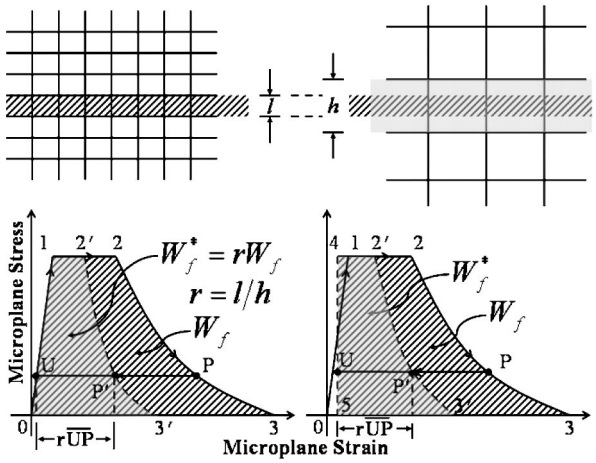


**Fig. 1.** (Top) Localized crack band; Adjustment of softening branches of microplane constitutive laws according to crack band model (proposed in Bažant et al. 2001); (bottom left) accurate method; (bottom right) simplified method

area 23542. Such rescaling is simpler and has been adopted for calculations.

Rescaling by this kind of affinity transformation is applied to tensile softening boundary of the statically constrained microplane system, which emulates the cohesive crack model for tension. It is also applied to each softening boundary in the kinematically constrained microplane system, i.e., to the softening positive and negative deviatoric boundaries, the tensile volumetric boundary, and the tensile normal boundary—the boundaries that control softening of the material in compression.

For a crack band running along the mesh lines of a rectangular or square mesh, $h$ represents the width of the elements forming the crack band. For a crack band running through an irregular mesh, $h$ cannot be defined exactly. However, it seems reasonable to simply assume that $h=4\times$ the ratio of the element area to the element perimeter, or $h=6\times$ the ratio of the element volume to its surface, in the case of two-or three-dimensional finite elements, respectively.

## Numerical Comparisons with Test Data

Although the present Model M5 has been verified by comparisons with all the test data used in verifying Model M4 (Caner and Bažant 2000), comparisons of the tests with compressive or compressive-shear loading need not be reproduced here because they are identical or almost identical. The only significant change, and the advantage of this model, is found in tensile fracturing tests reaching into very large tensile strains.

Two typical data sets have been selected for fitting—those of Petersson (1981) for uniaxial tension, and of Bresler and Pister (1958) for combined shear and uniaxial compression (produced by torsional–axial loading). The latter data represent the compression shear envelope. Its points have been obtained by running simulations of response for different ratios of axial normal stress and shear stress, and collecting the peak points. Optimum fitting of both these data has succeeded to produce a satisfactory match; see Figs. 2 and 3.

In Fig. 4, the effect of the load step size on the uniaxial tension response is shown. It is demonstrated in this figure that the model response is accurate with strain increments on the order of 1

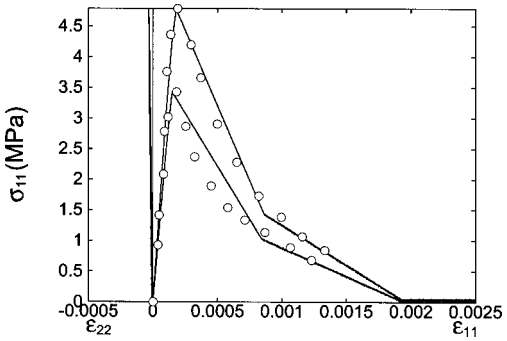


**Fig. 2.** Optimum fits of tensile softening test data of Petersson (1981), with corresponding lateral strain (data at bottom has compressive strength $f_c'=27$ MPa and other one $f_c'=41$ MPa); parameter values used in Model M5 are $k_1=0.000165$, $k_2=160$, $k_3=10$, $k_4=150$ with $\psi=0.3$, $\gamma_{N1}=0.005$, and $\gamma_{N2}=0.012$

$\times 10^{-5}$, just like its predecessors, despite the new algorithm which represents a radical improvement in the series of microplane models for concrete.

## Convergence Criteria for Series Coupling Model with Softening

Since the formulation of a convergent iterative algorithm has been the crucial step making the present series coupling model possible, a deeper analysis of the covergence problem is in order. It will be instructive to consider first an algorithm which comes to mind more naturally (and has in fact been tried long ago, albeit with disappointing results). Then we will try another algorithm and show why, and when, it works.

### *Algorithm A. Predictor of Positive Stiffness*

Consider a series coupling of two elements subjected to stress $\sigma$ (Fig. 1). As the applied load is reduced, one element, with strain $e$, unloads with a positive tangent stiffness $K$, and the other, with

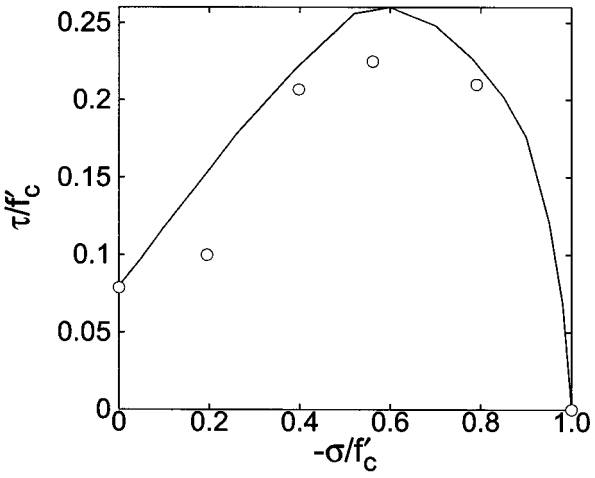


**Fig. 3.** Optimum fit of Bresler and Pister's (1958) test data for combined shear and uniaxial compression ($f_c'=68$ MPa); parameter values used in M5 are $k_1=0.0001$, $k_2=350$, $k_3=10$, $k_4=150$ with $\psi=0.3$, $\gamma_{N1}=0.005$, and $\gamma_{N2}=0.012$

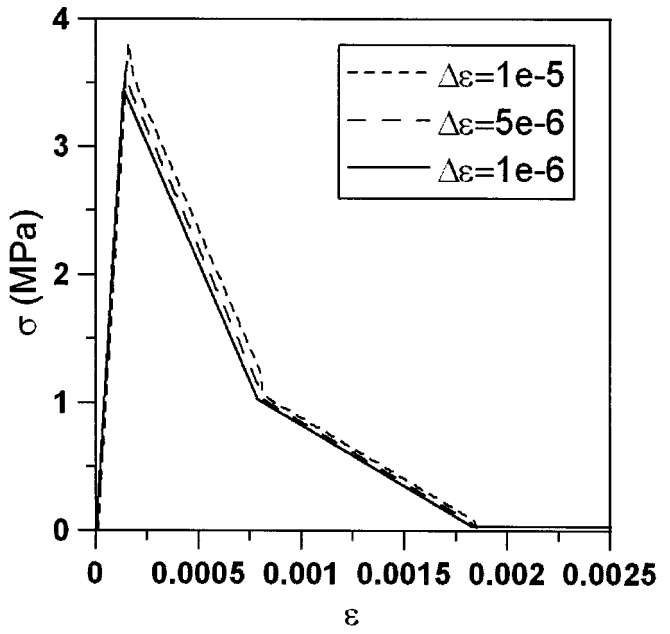


**Fig. 4.** Effect of loading step size in uniaxial tension response; the curve shown fits Petersson's data with $f_c'=27$ MPa already presented in Fig. 2

strain $\gamma=\epsilon-e$, expands with a negative tangent stiffness $K_t$ (i.e., is softening). Scalars $K$ and $K_t$, respectively, may be imagined as the overall tangential stiffnesses of the kinematically and statically constrained microplane systems for the actual direction of loading in the strain space.

In an iterative solution of the loading step, either $K$ or $K_t$ needs to be used as the predictor and the other as the corrector. In finite element programs for plasticity, the elastic deformation is used as the predictor, and the return to the current yield surface (i.e., the inelastic deformation) as the corrector. So, by analogy, it seems natural to use the positive (elastic) stiffness $K$ as the predictor, and the inelastic stiffness $K_t$ (a counterpart of the plastic hardening modulus) as the corrector. In this case, the algorithm of iterations (labeled by subscripts $i=1,2,3,\ldots$) for a given small step $\Delta\epsilon$ is as follows:

1. Denoting by subscript 0 the initial value at the beginning of the loading step, intialize either $\sigma_1=\sigma_0$ or $\sigma_1=\sigma_0+K\Delta e$, where $\Delta e$ is the increment obtained in the previous loading step (the latter reduces the necessary number of iterations if $\gamma$ varies smoothly).
2. Iteration loop, $n=1,2,3,\ldots N_{\text{it}}$; evaluate the predictor $\Delta\gamma=(\sigma_n-\sigma_0)/K_t$, and then the corrector $\sigma_{n+1}=\sigma_0+K(\epsilon-\epsilon_0-\Delta\gamma)$.
3. If the chosen tolerance is not met, reset $n\leftarrow n+1$, go to 2, and start a new iteration. Otherwise go to 1 and start the next loading step.

Overall, the algorithm leads to the following equation for the subsequent iterates $\sigma_n$:

$$\sigma_{n+1}+\frac{K}{K_t}\sigma_n=\left(1+\frac{K}{K_t}\right)\sigma_0+K(\epsilon-\epsilon_0) \tag{1}$$

This is a nonhomogeneous linear first-order difference equation with constant coefficients. It may be checked that its solution for initial value $\sigma_1$ is

$$\sigma_n=C\lambda^n+\sigma_\infty \tag{2}$$

with

$$\sigma_\infty=\sigma_0+\frac{\epsilon-\epsilon_0}{K^{-1}+K_t^{-1}},\qquad C=\frac{\sigma_1-\sigma_\infty}{\lambda} \tag{3}$$

Here $\lambda$, $\sigma_\infty$, and $C$=constant during the iterations; $\lambda$ is given by the characteristic equation $\lambda=-K/K_t$; and $\lambda>0$ for the postpeak. The iterations will converge if and only if $\lim_{n\to\infty}\lambda^n=0$, i.e., $|\lambda|<1$. So we conclude that an algorithm in which the positive stiffness is the predictor will converge if and only if

$$|K_t|>K$$

or

$$K_t<-K \tag{4}$$

Since the value of $K_t$ may decrease continuously as $\epsilon$ increases during loading, we conclude that this iterative algorithm will inevitably diverge at least for the initial postpeak softening, if not always. This is unacceptable. Thus we arrive at a conclusion that might at first seem surprising: An algorithm analogous to the standard iterative algorithm with return to the yield surface, as used in incremental plastic finite element analysis, is impossible.

### *Algorithm B. Fracture-Based Predictor*

Let us now explore an algorithm for which, in contrast to plastic finite element analysis, the negative stiffness $K_t$ for the inelastic (fracturing) part $\gamma$ of the total strain $\epsilon$ (Fig. 1) is used as the predictor, and $K$ as the corrector. The algorithm for a given small loading step $\Delta\epsilon$ is as follows:

1. Either set $\Delta e_1=0$ or use for $\Delta e_1$ the value obtained in the preceding loading step (the latter shortens the iterations provided that $e$ can be expected to evolve smoothly).
2. Iteration loop, $n=1,2,3,\ldots$; evaluate the predictor $\Delta\sigma=K_t(\Delta\epsilon-\Delta e_n)$ and then the corrector $e_{n+1}=\Delta\sigma_n/K$.
3. If the chosen tolerance is not met, reset $n\leftarrow n+1$, go to 2, and start a new iteration. Otherwise go to 1 and start the next loading step.

Overall, the algorithm leads to the following equation for the subsequent iterates $\Delta e_n$:

$$\Delta e_{n+1}+\frac{K_t}{K}\Delta e_n=\frac{K_t}{K}\Delta\epsilon \tag{5}$$

This is again a nonhomogeneous linear first-order difference equation with constant coefficients. It may be checked by substitution that its solution for initial value $\Delta e_1$ is

$$\Delta e_n=C\lambda^n+\Delta e_\infty \tag{6}$$

with

$$\Delta e_\infty=\frac{K}{K+K_t}\Delta\epsilon,\qquad C=\frac{\Delta e_1-\Delta e_\infty}{\lambda} \tag{7}$$

Here $\lambda$, $\Delta e_\infty$, and $C$=constant during the iterations, and $\lambda$ is given by the characteristic equation $K\lambda+K_t=0$, i.e., $\lambda=-K_t/K$. The it-

erations will converge if and only if $\lim_{n\to\infty}\lambda^n=0$, i.e., $|\lambda|<1$ or

$$|K_t|<K$$

or

$$K_t>-K \tag{8}$$

which is opposite to inequality (4). We thus conclude that, for postpeak softening, this iterative algorithm will work, unless the softening stiffness magnitude exceeds the elastic stiffness. The subsequent iterates form a geometric progression, and so the convergence is exponential.

Should we fear that inequality (8) might become violated for the normal behavior of concrete? To answer this question, consider the typical values $f_t'=3$ MPa, $G_f=30$ N/$n$ (fracture energy corresponding to the initial tangent of the softening stress–separation curve of the cohesive crack model (Bažant 2002a,b), and average crack spacing $s=50$ mm. This furnishes for the average softening modulus for tensile cracking concrete the estimate $|K_t|=f_t'^2s/2G_f=7.5$ GPa, while the typical value of elastic modulus is $K\approx 26$ GPa, which is much higher than 7.5 GPa. Therefore, the limiting postpeak softening tangent modulus $K_t$ for which the convergence of this algorithm would be lost will hardly ever be reached, for normal concrete and normal crack spacing. If inequality (8) is violated, one must question whether the considered crack spacing $s$ is realistic. Reducing $s$ causes a decrease of $|K_t|$ and thus helps convergence (just like reducing the finite element size in the crack band model).

### Can Convergence Be Accelerated?

To accelerate convergence, one may try replacing the predictor in Step 2 of algorithm B, beginning with the third iteration ($n>2$), by $\Delta\sigma=K_t[\Delta\epsilon-\Delta e_n-\alpha(\Delta e_n-\Delta e_{n-1})]$, where $\alpha$ is an empirically chosen acceleration factor; $\alpha\in(0,1)$ might be expected to accelerate monotonic convergence, and $\alpha\in(-1,0)$ oscillatory convergence. The algorithm then leads (for $n>2$) to the equation

$$K\Delta e_{n+1}+K_t(1+\alpha)\Delta e_n-K_t\alpha\Delta e_{n-1}=K_t\Delta\epsilon \tag{9}$$

This is a nonhomogeneous linear second-order difference equation with constant coefficients. Solutions of its homogeneous part may be sought in the form $\Delta e_n=C\lambda^n$. Substituting this into Eq. (9), one gets the characteristic equation $K\lambda^2+(1+\alpha)K_t\lambda-\alpha K_t=0$, which has two roots

$$\left.\begin{matrix}\lambda_1\\ \lambda_2\end{matrix}\right\}=\frac{(1+\alpha)K_t}{2K}\left(-1\pm\sqrt{1+\frac{4\alpha K}{(1+\alpha)^2K_t}}\right) \tag{10}$$

The solution has the general form $\Delta e_{n+1}=C_1\lambda_1^n+C_2\lambda_2^n+\Delta e_\infty$, where $\Delta e_\infty$ is the same as before and constants $C_1$ and $C_2$ must be solved from the initial $\Delta e_n$ values for $n=1,2$. Now we observe that, if $a>0$, both roots are negative, but in that case a convergence acceleration would necessitate $\lambda<0$, a contradiction. If $\alpha<0$ (but not of a magnitude large enough to produce a complex root) $\lambda_1$ is positive, which calls for $\alpha>0$ but $\lambda_2$ is negative, which calls for $\alpha<0$, and so acceleration cannot be guaranteed. Therefore, a significant convergence acceleration with factor $\alpha$ seems, in general, unattainable.

There is, however, another way to accelerate convergence—use the Newton-Raphson algorithm, based on transential stiffness matrices of the statically and binematically constrained systems. It so happens that in the microplane model, they can be easily determined from microplane tangent stiffnesses.

### Tensorial Analysis of Convergence of Algorithm B

Strictly speaking, the preceding analysis of convergence of algorithms A and B is valid only when Matrix $K_t$ does not change from one iteration to the next. In general, it may change because the loading direction in the strain space need not be fixed but can rotate. Then the cnvergence must be analyzed tensorially. The generalized tensorial form of iterative algorithm B for a small loading step $\Delta\varepsilon$ reads, for $\alpha=0$, as follows:

1. Either set $\Delta\boldsymbol{e}_1=\mathbf{0}$ or use for $\Delta\boldsymbol{e}_1$ the tensorial increment obtained in the preceding loading step (the latter shortens the iterations provided that $\boldsymbol{e}$ can be expected to evolve smoothly).
2. Iteration loop, $n=1,2,3,\ldots$; Evaluate predictor $\Delta\boldsymbol{\sigma}=\boldsymbol{K}_t:[\Delta\boldsymbol{\varepsilon}-\Delta\boldsymbol{e}_n-\alpha(\Delta\boldsymbol{e}_n-\Delta\boldsymbol{e}_{n-1})]$, and then solve the corrector $\boldsymbol{e}_{n+1}$ from the equation $\Delta\boldsymbol{\sigma}_n=\boldsymbol{K}:\boldsymbol{e}_{n+1}$ (where the colon denotes a doubly contracted tensorial pruduct).
3. If the chosen tolerance is not met, reset $n\leftarrow n+1$, go to 2, and start a new iteration. Otherwise go to 1 and start the next loading step.

Overall, when all the vectors and second-order symmetiric tensors (denoted by italic bold letters and by $\boldsymbol{\epsilon}$) are replaced by $6\times1$ and $6\times6$ matrices (denoted by roman bold letters and by $\boldsymbol{\varepsilon}$), the algorithm leads to the following matrix equation for the subsequent iterates $\Delta\mathbf{e}_n$:

$$\Delta\mathbf{e}_{n+1}-\mathbf{A}\Delta\mathbf{e}_n=-\mathbf{A}\Delta\boldsymbol{\epsilon},\quad\text{with}\quad\mathbf{A}=-\mathbf{K}^{-1}\mathbf{K}_t \tag{11}$$

This is a nonhomogenous linear first-order matrix difference equation with constant matrix coefficients. It may be checked that its solution for initial value $\Delta\mathbf{e}_1$ is

$$\Delta\mathbf{e}_n=\mathbf{A}^n\mathbf{C}+\Delta\mathbf{e}_\infty \tag{12}$$

where

$$\Delta\mathbf{e}_\infty=-(\mathbf{I}-\mathbf{A})^{-1}\mathbf{A}\Delta\boldsymbol{\epsilon},\qquad\mathbf{C}=\mathbf{A}^{-1}(\Delta\mathbf{e}_1-\Delta\mathbf{e}_\infty) \tag{13}$$

in which $\mathbf{A}$, $\mathbf{C}$, and $\Delta\mathbf{e}_\infty$=constant square and column matrices during the iterations, and $\mathbf{I}$=unit $6\times6$ matrix.

To discuss convergence, consider that the coordinates are rotated (in a six-dimensional space), by rotation Matrix $\mathbf{R}$, into the principal directions of Matrix $\mathbf{K}$ (not to be confused with the principal directions of stress or strain tensor in three dimensions). We may also assume that the principal directions of Matrix $\mathbf{K_t}$ (in six dimensions) are the same. Then, in the principal coordinates, Matrix $\mathbf{A}$ becomes

$$\mathbf{A}'=\mathbf{R}^{\mathbf{T}}\mathbf{A}\mathbf{R}=\begin{bmatrix}K_1^{-1}&&&\\&K_2^{-1}&&\\&&\cdots&\\&&&K_6^{-1}\end{bmatrix}\begin{bmatrix}-K_{t1}&&&\\&-K_{t2}&&\\&&\cdots&\\&&&-K_{t6}\end{bmatrix}=\begin{bmatrix}\lambda_1&&&\\&\lambda_2&&\\&&\cdots&\\&&&\lambda_6\end{bmatrix} \tag{14}$$

where

$$\lambda_1=-K_1^{-1}K_{t1},\quad\lambda_2=-K_2^{-1}K_{t2},\ldots\lambda_6=-K_6^{-1}K_{t6} \tag{15}$$

Here $K_1,K_2,\ldots K_6$=eigenvalues of Matrix $\mathbf{K}$, and $K_{t1}$, $K_{t2},\ldots K_{t6}$=eigenvalues of Matrix $\mathbf{K}_t$. The iterations will converge if and only if $\lim_{n\to\infty}\mathbf{A}^n=\lim_{n\to\infty}\mathbf{A}'^n=\mathbf{0}$; i.e., all

$|\lambda_1|, |\lambda_2|, \ldots |\lambda_6|$ must be less than 1. This requires that

$$|K_{t1}| < K_1,$$
$$|K_{t2}| < K_2, \ldots |K_{t6}| < K_6 \tag{16}$$

Thus we have demonstrated tensorially that the iterative algorithm will converge if and only if each principal value of the tangent stiffness matrix for softening is smaller in magnitude than the corresponding principal value of the elastic stiffness matrix. The subsequent iterates form a matrix geometric progression.

## Detailed Explicit Algorithm for M5

Finally, to permit unambiguous programming of the present model, the complete detailed algorithm for step-by-step loading will now be given. The strains and stresses at the beginning of each small loading step are known, and the material subroutine must deliver the stress tensor corresponding to a given strain tensor (and update the microplane history variables such as the maximum strain achieved so far). The stress tensor at various integration points is then used in numerical integration over the finite element to obtain the internal force vector of the element, and all these vectors from all the finite elements are then assembled to furnish the internal force vector of the structure.

The type of finite element program will decide when the microplane history variables should be updated. When the finite element program is explicit, these variables will be updated at the end of every time integration step. An implicit finite element program, on the other hand, will check whether convergence has been achieved, and only then it will update these variables. Once these microplane variables are updated, the stress tensor returned along with every other variable calculated in the finite element program using these stress components becomes validated.

The values of **n**, **m**, and $l$ for each microplane are input in advance of finite element analysis and used to calculate tensors $N_{ij}=n_i n_j$, $M_{ij}=\text{sym}\ n_i m_j$, and $L_{ij}=\text{sym}\ n_i l_j$. These tensors are then stored to be used in structural analysis. The algorithm for the material subroutine is as follows:

1. The (macro)-strains $\epsilon_{ij}$ and their increments $\Delta\epsilon_{ij}$ are given. The microplane history stresses of the modified Model M4, $s_N^0$, $s_L^0$, and $s_M^0$, are stored for each microplane and $s_V^0$ is stored for all microplanes in the previously converged load step. Similarly, the microplane history strains of the statically constrained microplane model with cohesive law, $\gamma_N^0$, $\gamma_N^0$, and $\gamma_M^0$, are stored for each microplane in that step.
2. Set tolerance $=1\times10^{-12}$. Then reconstruct $\gamma_{ij}$ and $s_{ij}$ from the history variables via numerical integration of history variables:

$$\gamma_{ij} = \frac{3}{2\pi}\int_\Omega (\gamma_N^0 N_{ij} + \gamma_M^0 M_{ij} + \gamma_L^0 L_{ij}) d\Omega \tag{17}$$

$$s_{ij} = \frac{3}{2\pi}\int_\Omega \left[ s_D^0\left(N_{ij} - \frac{\delta_{ij}}{3}\right) + s_M^0 M_{ij} + s_L^0 L_{ij}\right] d\Omega + s_V^0\delta_{ij} \tag{18}$$

3. Calculate $e_{ij}=\epsilon_{ij}-\gamma_{ij}$.
4. Compute the fracturing compliance, $C_{ijkl}^f$, and the current error in the additive split of increment of total strain, $r_{ij}$, that must be minimized as follows:
   (a) Using elastic stiffness Matrix $K$, compute the predictor $\Delta\sigma_{ij}=K_{ijkl}\Delta e_{kl}$;
   (b) Using static constraint, calculate the microplane stress increments: $\Delta\sigma_N=N_{ij}\Delta\sigma_{ij}$, $\Delta\sigma_M=M_{ij}\Delta\sigma_{ij}$, and $\Delta\sigma_L=L_{ij}\sigma_{ij}$;
   (c) The predicted total stress tensor now becomes $\sigma_{ij}=s_{ij}+\Delta\sigma_{ij}$ and, using the static constraint, the microplane stresses are calculated: $\sigma_N=N_{ij}\sigma_{ij}$, $\sigma_M=M_{ij}\sigma_{ij}$, and $\sigma_L=L_{ij}\sigma_{ij}$. Thereupon, the crack opening at all microplanes can be evaluated.
   i. Check whether $\gamma_N^0<1\times10^{-10}$; if true, set $\gamma_N^0=1\times10^{-10}$. Similarly, if $|\gamma_M^0|<1\times10^{-10}$ then set $\gamma_M^0=1\times10^{-10}\ \text{sgn}(\gamma_M^0)$, and if $|\gamma_L^0|=1\times10^{-10}$ then $\gamma_L^0=1\times10^{-10}\ \text{sgn}(\gamma_L^0)$.
   ii. Compute $\sigma=[\sigma_N^2+(\sigma_M^2+\sigma_L^2)\beta^{-2}]^{1/2}$. If $\sigma\neq0$ then $\Delta\sigma=[\Delta\sigma_N\sigma_N+(\Delta\sigma_M\sigma_M+\Delta\sigma_L\sigma_L)\beta^{-2}]/\sigma$, or else $\Delta\sigma=[\Delta\sigma_N^2+(\Delta\sigma_M^2+\Delta\sigma_L^2)\beta^{-2}]^{1/2}$, $\gamma^0=\{(\gamma_N^0)^2+[(\gamma_M^0)^2+(\gamma_L^0)^2]\beta^2\}^{1/2}$, and $\sigma^0=\sigma-\Delta\sigma$.
   iii. Set $Small=1\times10^{-2}f_t'$. For all microplanes, check if $\sigma+Small\leqslant0$, if true, set $\gamma_N=\gamma_M=\gamma_L=1\times10^{-10}$. Then calculate the elastic compliance $C=\min(\max(\gamma^0/\sigma^0,1\times10^{-5}),100)$. If $\sigma+Small>0$, calculate the cohesive law stress $\sigma^b$ using Eqs. (16) of Part I at $\gamma=\gamma^0$. Also choose $0\leqslant k_u\leqslant1$.
   iv. Compute $\Delta\sigma^*=\sigma-\sigma^b$. If $\Delta\sigma^*>0$, first compute.

$$\gamma = \gamma^0 + \left(-\frac{\psi f_t'}{\gamma_{N2}-\gamma_{N1}}\right)\Delta\sigma^* \tag{19}$$

   and then calculate the fracturing compliances

$$C_N^f = \gamma/\sigma;$$
$$C_M^f = C_L^f = \beta^{-2}\gamma/\sigma \tag{20}$$

   v. If $\Delta\sigma^*\leqslant0$, calculate $\gamma=\gamma^0+k_u C\Delta\sigma$, Then compute $\gamma_N=\gamma\ \sigma_N/\sigma$, $\gamma_M=\gamma_{\sigma_M}/\sigma$, and $\gamma_L=\gamma\sigma_L/\sigma$; furthermore set the microplane fracturing compliances $C_N^f=C_M^f=C_L^f=Small$ for all microplanes.
   (d) Now calculate the predicted strain tensor increment by numerical integration:

$$\Delta_{\gamma_{ij}} = \frac{3}{2\pi}\int_\Omega (\gamma_N N_{ij} + \gamma_M M_{ij} + \gamma_L L_{ij}) d\Omega - \gamma_{ij} \tag{21}$$

   (e) Thus one arrives at the prediction of the current error in the additive split of increment of strain as $r_{ij}=-\Delta e_{ij}-\Delta\gamma_{ij}+\Delta\epsilon_{ij}$
   (f) Finally, the fracturing compliance tensor $C_{ijkl}^f$ can be calculated as the integration of microplane compliances over the unit hemisphere

$$C_{ijkl}^f = \frac{3}{2\pi}\int_\Omega (C_N^f N_{ij}N_{kl} + C_M^f M_{ij}M_{kl} + C_L^f L_{ij}L_{kl}) d\Omega \tag{22}$$

5. It is convenient to adopt Voigt notation in what follows. In order to minimize the error $r_i$, $(i=1,2,\ldots6)$, its gradient is needed. It can be expressed in the Voigt notation as $G_{ij}=-C_{\text{in}}^f K_{nj}-\delta_{ij}(i,j,n=1,2,\ldots6)$ [see Eq. (13) in Part I], and it needs to be calculated only once when the equilibrium solution is achieved.
6. Set $\Delta e_i=0$, $(i=1,2,\ldots6)$ and implement a Newton–Raphson iterative algorithm in order to determine $\Delta e_i$ that minimizes the error $r_i$ by looping over the following steps:

(a) Calculate the error $r_i = r_i(\Delta e_i)$ for a given total strain increment $\Delta\epsilon_i$ using Steps 4a through 4b; (b) compute $\delta\Delta e_i = -G_{in}^{-1} r_n$ and replace $\Delta e_i$ by $\Delta e_i + \delta\Delta e_i$; and (c) calculate the error magnitude as $\xi = (r_i r_i)^{1/2}$ and continue the loop until $\xi \leqslant$ tolerance. Typically tolerance $\approx 1 \times 10^{-3}$ for convergence at the initiation of the choesive fracture due to sudden onset of softening, and tolerance $1 \times 10^{-12}$ at all other times.

7. Switching back to tensor notation, apply the kinematic constraint to get the microplane strain components $\Delta e_N = N_{ij}\Delta e_{ij}$, $\Delta e_V = \Delta e_{kk}/3$, $\Delta e_D = \Delta e_N - \Delta e_V$, $\Delta e_L = L_{ij}\Delta e_{ij}$, $\Delta e_M = M_{ij}\Delta e_{ij}$.
8. Check the loading criteria $s_V \Delta e_V > 0$, $s_D \Delta e_D > 0$, $s_T \Delta e_T > 0$ if loading, $s_V \Delta e_V \leqslant 0$, $s_D \Delta e_D \leqslant 0$, $s_T \Delta e_T \leqslant 0$ if unloading, and decide the value of the incremental elastic modulus on each microplane.
9. Compute $s_V^e = s_V^0 + E_V \Delta e_V$ and the boundary value $s_V^{b-} = F_V^-(-e_V)$; set

$$s_V^* = \max(s_V^{b-}, s_V^e) \tag{23}$$

10. Compute $s_D^e = s_D^0 + E_D \Delta e_D$ and the boundary values $s_D^{b-} = F_D^-(e_D)$ and also $s_D^{b+} = F_D^+(e_D)$; calculate

$$s_D = \min[\max(s_D^{b-}, s_D^e), s_D^{b+}] \tag{24}$$

11. For each microplane, compute $s_N = s_V^* + s_D$, and also $s_N$ at the boundary as $s_N^b = F_N(e_N)$. But, to prevent violating the normal boundary, set

$$s_N = \min(s_N, s_N^b) \tag{25}$$

12. Recalculate $s_V$ as the average of the microplane normal stress $s_N$ over the surface of the unit hemisphere. But to prevent this value from exceeding the volumetric stress calculated in item 9 as $s_V^*$, set

$$s_V = \min\left( \int_\Omega s_N \, d\Omega/2\pi, \; s_V^* \right) \tag{26}$$

13. Recalculate $s_D = s_N - s_V$ for each microplane.
14. Calculate the shear stress at the boundary as $s_T^b = F_T(s_N)$ and the elastic shear stresses as $s_L^e = s_L^0 + E_T \Delta e_L$ and $s_M^e = s_M^0 + E_T \Delta e_M$; then, determine the shear stresses in $\boldsymbol{l}$ and $\boldsymbol{m}$ directions, respectively, as $s_L = \text{sgn}(s_L^e)\, \min(|s_T^b|, |s_L^e|)$ and $s_M = \text{sgn}(s_M^e)\, \min(|s_T^b|, |s_M^e|)$.
15. Compute the components of the (macro)-stress tensor by numerical integration over a unit hemisphere

$$s_{ij} = \frac{3}{2\pi} \int_\Omega \left[ s_D \left( N_{ij} - \frac{\delta_{ij}}{3} \right) + s_M M_{ij} + s_L L_{ij} \right] d\Omega + s_V \delta_{ij} \tag{27}$$

16. Return stress tensor $s_{ij}$ and history variables $s_N$, $s_M$, $s_L$, $s_V$, $\gamma_N$, $\gamma_M$, and $\gamma_L$ to the finite element program.

It might seem that, as an alternative, one could calculate the error $\xi$ in Step 6c in terms of $\Delta s_{ij}$, and if the tolerance were not satisfied, set $\Delta s_{ij}^{\text{pre}} = \Delta s_{ij}$, after which $\Delta s_{ij}^{\text{pre}}$ could be used in Step 4c. However, such an algorithm is found to diverge shortly after tensile softening begins.

Thanks to the inclusion of the Newton–Raphson algorithm in Step 6, strain increments as large as $2 \times 10^{-5}$ gave accurate results. Initially, this algorithm was not included, and then strain increments as small as $10^{-8}$ had to be used to achieve good accuracy when steep tensile softening (or cracking) was in progress.

## Conclusions

1. Microplane Model M5 achieves as realistic representation of progressive tensile cracking or cohesive fracture. It avoids stress locking and spurious excessive lateral contraction or expansion at very large postpeak tensile strains.
2. This improvement is achieved by a series coupling of two microplane systems: one constrained kinematically and the other statically. The latter simulates exclusively tensile cracking and fracture, while the former simulates all the nonlinear triaxial behavior in pure compression and compression with shear.
3. The coupling of two microplane systems in made possible by developing a new iterative algorithm which avoids solving the implicit nonlinear equations that relate the two microplane systems.
4. A special characteristic of this algorithm is that, in each loading step, the softening cohesive fracture properties of the statically constrained microplanes are used as the predictor and the hardening or properties of the kinematically microplanes are used as the corrector that returns the current state point to the stress–strain boundaries (softening yield limits). The roles of predictor and corrector are interchanged compared to the classical iterative returns mapping algorithms for hardening elasto–plastic behavior.
5. It is proven that the new iterative algorithm converges in a geometric progression, and the conditions of convergence are derived.
6. Except for a few minor differences, the constitutive properties on the kinematically constrained microplanes are the same as in the previous Model M4. In other words, except for tensile softening, the response is the same.
7. Further acceleration, with quadratic convergence, is achieved by using Newton-Raphson iterations to determine the strain subdivision between the two microplane systems. This is made possible by determining the tangential stiffnesses on that microplane level.
8. The softening cohesive fracture properties are related to the fracture energy and effective crack spacing in the same manner as in the preceding improved version M4f of microplane Model M4. The postpeak softening slope on the microplanes can be adjusted in the sense of the crack band model, to ensure the correct energy dissipation of localized fracture when the finite element size is varied.
9. The constitutive properties that differ from Model M4 are shown to allow good representation of test data for tensile softening of concrete and of the shear-compression failure envelope of concrete.
10. An incremental thermodynamic potential for the coupling of statically and kinematically constrained microplane models is formulated. If represents a combination of the Helmholtz and Gibbs free energy densities.

## Acknowledgments

Parts I and II of this study were partially funded under Grant No. CMS-0732791 from the U.S. National Science Foundation and Grant No. DE-FG07-98ER45736 from the Department of Energy, made both to Northwestern University.

## References


Bažant, Z. P. (1976), "Instability, ductility, and size effect in strain-softening concrete." *J. Eng. Mech. Div.,* 102(2), 331–344.

Bažant, Z. P. (2002a). *Scaling of structural strength*, Hermes Science, London.

Bažant, Z. P. (2002b). "Concrete fracture models: Testing and practice." *Eng. Fract. Mech.,* 69(2), 165-206.

Bažant, Z. P., and Caner, F. C. (2005). "Microplane model M5 with kinematic and static constraints for concrete fracture and anelasticity. I. Theory." *J. Eng. Mech.,* 131(1), 31–40.

Bažant, Z. P., Červenka, J., and Wierer, M. (2001). "Equivalent localization element for crack band model and as alternative to elements with embedded discontinuities." *Proc., 4th Int. Conf. Fracture Mechanics of Concrete Structures Paris*, R. de Borst et al., eds., Swets & Zeitlinger, A. A. Balkema, Lisse, The Netherlands, 765–772.

Bažant, Z. P., Červenka, J., and Wierer, M. (2001b). "Equivalent localization element for crack band approach to mesh-size sensitivity in microplane model." *Int. J. Numer. Methods Eng.* (in press).

Bažant, Z. P., and Oh, B.-H. (1983). "Crack band theory for fracture of concrete." *Mater. Struct.,* 16, 155–177.

Bažant, Z. P., Zi, G., and Jendele, L. (2002). "Softening adjustment of microplane model M4 based on fracture energy and crack band theory: Model M4f for Code ATENA." Private Communication to Dr. Jan Červenka, Červenka Company, Prague.

Bresler, B., and Pister, K. S. (1958). "Strength of concrete under combined stresses." *J. Am. Concr. Inst.,* 55(20), 321–345.

Caner, F. C., and Bažant, Z. P. (2000). "Microplane model M4 for concrete: II. Algorithm and calibration." *J. Eng. Mech.,* 126(9), 954–961.

Petersson, P. E. (1981). "Crack growth and development of fracture zones in plain concrete and similar materials." *Rep. No. TVBM 1006*, Lund Inst. of Technology, Lund, Sweden.